Polymer Bulletin 41, 615–622 (1998)

Polymer Bulletin
© Springer-Verlag 1998

Low-rate fracture behaviour of magnesium hydroxide filled polypropylene block copolymer

J. I. Velasco[1,*] C. Morhain[2], D. Arencón[2], O. O. Santana[2], M. L. Maspoch[1]

[1] Departament de Ciencies dels Materals i Enginyeria Metallúrgica, Universitat Politècnica de Catalunya, Avenida Diagonal 647, E-08028 Barcelona, Spain
[2] Centre Català del Plàstic, C/Colom 114, E-08222 Terrassa, Spain

Received: 22 July 1998/Revised version: 6 October 1998/Accepted: 6 October 1998

Summary

This paper presents the fracture behaviour of injection-moulded magnesium hydroxide filled polypropylene block copolymer (PP) as a function of the filler content, and it is compared to that of the unfilled PP. The *J*-integral concept was applied from tests carried out on SENB specimens according to the European Structural Integrity Society (ESIS) protocol for plastics. The results show lower fracture toughness (J_{IC}) as the filler content increases in the composite, what is explained on the basis of morphological details.

Introduction

Nowadays, magnesium hydroxide is employed as an effective halogen and acid-free flame retardant and smoke suppressing additive for polypropylene [1]. Magnesium hydroxide decomposition starts at 300 °C, a high enough temperature to enable the material to be compounded successfully into most polymers:

$$Mg(OH)2 \longrightarrow MgO + H2O - 1450\ J/g$$

As a result, the polymer is cooled and thus fewer pyrolysis products are formed. The combustion products of $Mg(OH)_2$/PP composites are neither toxic nor corrosive. Along with the charring products, the MgO formed on the surface of the substrate acts as an insulating protective layer. Moreover, the water vapour released has a diluting effect in the gas phase and forms an oxygen-displacing protective layer over the condensed phase. Chemical reactions such as interruption of the radical chain mechanism of the gas phase combustion processes have not been detected.

A satisfactory flame retardancy of PP requires very high contents of this filler, which promotes important changes in its mechanical properties, limiting its practical applications.

In contrast to the quite well known elastic properties of particulate filled PP composites, few studies dealing with the composition dependence of the fracture toughness of particulate filled composites has been published [2-4].

The aim of the present work is to study the fracture behaviour of magnesium hydroxide filled polypropylene copolymer at low strain rate. Since PP copolymer presents a broad range of non-linearity in its stress/strain behaviour, the fracture toughness has been characterised by an approximation of the J-integral concept based on the construction of the resistance *J-R* curve [5].

Experimental

Materials and specimens

A commercial grade (*Magnifin H5L*) of magnesium hydroxide, supplied by *Martinswerk GmbH*, was used in this work. It was a high purity mineral with well-defined hexagonal platy particles, having a mean particle size of 1.4 μm. The polypropylene employed was a

* Corresponding author

commercial PP block copolymer (*Isplen PB140*), supplied by *Repsol Química S.A.*, suitable for the manufacture of technical products by injection moulding.
Compounding was performed using a *Collin* co-rotating twin-screw extruder. The screw diameter was 24 mm and its length/diameter ratio was 25. The process was carried out with the following temperature profile: 140, 180, 185, 190, 195 °C. The screw speed was fixed at 60 rpm, and an optimal dispersion of the $Mg(OH)_2$ particles into the PP matrix was achieved by the following screw configuration: two compression zones on both sides of a mixing zone constituted by double-tipped kneading elements. A circular cross-section die of diameter 3-mm was employed, and the extrudate was cooled in water and pelletised. By this way two composites were prepared with filler concentrations of 40wt% (PP40) and 60wt% (PP60) respectively. The unfilled PP was also subjected to the same extrusion process in order to get the same thermal and mechanical histories in each material. The initial characteristics of the samples are given in Table 1.
Standard tensile specimens (type "I" according to ASTM D 638) and prismatic bars with nominal dimensions 6.35 x 12.7 x 127 mm^3 were injection-moulded using a *Mateu-Solé* 440/90 injection moulding machine and a multiple cavity mould, as described in figure 4 of the ASTM D-647 standard. The nominal injection pressure was 100 MPa and the temperature of the melt 195 °C. Before the tests, all the specimens were annealed at 110 °C during 18 hours in order to release the residual stresses. Any deformed specimens were rejected.

Testing procedure
A tensile characterisation was carried out at three different crosshead speeds: 1, 10 and 100 mm/min.
J-integral fracture tests were conducted by applying the multiple specimen technique on single edge notched bend (SENB) specimens at a speed of 1 mm/min, according to the ESIS protocol for plastic materials [6]. The specimens dimensions were $b \times D \times L$ = 6.35 x 12.7 x 63.5 mm^3, and they were obtained by cutting the injected bars into halves. To obtain the SENB geometry a notch was inserted centrally on the narrowest side of each specimen, using a 45° V notch broaching tool with a notch tip radius of 0.25 mm. These blunt notches were then sharpened with a single cut from a razor blade in order to get an initial sharp crack of 6.35 mm depth (a_0), and therefore to get an a_0/D = 0.5 ratio. The relation between the span (S) and the specimen width (D) was 4.

Table 1. Initial characterisation of the samples.

Material	[1] *Particles weight fraction*	[2] *Particles volume fraction*	[3] *Melt Flow Index*	[4] *Heat deflection temperature*
	W_p (%)	V_p (%)	*MFI* (g/10 min)	*HDT* (° C)
PP	0	0	3.3	54
PP40	40	20	3.2	67
PP60	60	36	1.6	74

[1] From burning test, [2] from density measurements, [3] measured at 230 ° C and 2160 g, [4] measured at 120 ° C/h and 1.8 MPa.

For SENB specimens with S/D = 4 the fracture resistance (J) allowing for crack growth may be calculated (6) by:

(1) $$J = J_0\left[1 - \frac{\Delta a}{2\,(D - a_0)}\right]$$

with

(2) $$J_0 = \frac{2U}{b\,(D - a_0)}$$

where U represents the energy to initiate and propagate the crack. To construct the *J-R* (J-Δa) curves, a set of identical SENB specimens with a_0 = 6.35 mm were loaded monotonically to different deflections, all less than that to give total failure, to obtain different levels of stable crack extension (Δa), and then fully unloaded. For each specimen, the J value was calculated from the energy until that deflection (U) using equation (1). The energy (U) was taken as the area under the load-displacement curve after having subtracted the indentation energy contribution.

To develop the stable crack extension (Δa) in each specimen, it was necessary to put a drop of Indian ink into the initial crack tip before loading. Once the ink had dried, the specimens were fractured by impact and so the ink on the fracture face developed the stable crack growth. Measurement of the final crack front from the fracture face was carried out using an optical microscope.

The experimental J-Δa data were fitted using a power law approximation:

(3) $$J = C_1\,\Delta a^{C_2}$$

Crack growth initiation occurs at a critical value (J_{IC}) of the J-integral, and in tough materials like PP an initial pseudo-extension of crack occurs, which is due to crack tip blunting. To consider this effect a crack blunting line is traditionally used [7]:

(4) $$J = 2\,\sigma_y \Delta a$$

where σ_y is the material yield stress. Here, the critical value (J_{IC}) is given by the intersection of the power law fitted (J-Δa) curve (eq. 3) and the blunting line (eq. 4), and it is compared with the $J_{0.2}$ value, which is also suggested as a fracture criterion by the ESIS [6]. Once J_{IC} has been exceeded, the resistance to crack propagation may be characterised by the value of the tearing modulus (T_M) [8]:

(5) $$T_M = \frac{E}{\sigma_y^2}\frac{dJ}{d\Delta a}$$

which essentially depends on the slope of the resistance *J-R* curve.

The geometric condition $D = 2b$ maximises the opportunity to obtain plane-strain conditions at the crack tip. This is the approach used conventionally for metals and it has been employed successfully when carried out LEFM tests on plastics. To measure the material yield stress under similar geometric conditions to those applied in the J-integral fracture tests, and ideally under plane strain conditions, three point bend (TPB) tests were also carried out on the unnotched prismatic specimens and at the same speed of 1 mm/min. The modulus of elasticity (E^{TPB}) and the yield stress (σ_y^{TPB}) were measured.

All the tests were performed at room temperature using an *Adamel DY-34* universal testing machine. The strain values in the tensile tests were measured using a *Hounsfield 500-L* optical extensometer.

Fractography

To investigate the morphological aspects associated with the fracture process, the fracture surfaces were examined by scanning electronic microscopy (SEM), using a *Jeol JSM-820* equipment, after coating the samples with a thin gold layer.

Results and discussion

Tensile behaviour

In Fig. 1 tensile stress/strain curves of PP and PP/Mg(OH)2 composites are compared, and information on the Young's modulus (E) and on the tensile yield stress (σ_y) of the materials is given in Table 2. The Young's modulus was obtained from the slope of the initial elastic zone of the stress/strain curve, and the tensile yield stress was considered as the maximum stress of the curve. The results show that the stiffness of the composite increases as the Mg(OH)2 content does as it is expected form the higher relative stiffness of the mineral respective to the polymer. The tensile yield stress and the strain at yield and at break of the polypropylene decreased when filled with Mg(OH)2. This must be associated with a weak particle/matrix interface in the composites, which promote particle debonding at low stress levels, what reduce the specimen effective cross-section and so the yield stress. The dispersed particles of Mg(OH)2 act limiting the plastic flow of the PP matrix and promoting an early failure of the specimen, which results in low values of elongation at break. Due to the PP viscoelasticity, both the Young's modulus and the yield stress increased with the test speed.

Although the Mg(OH)2 particles used in this work have not a spherical shape, their mean aspect ratio is quite small (~5) and, therefore, the measured Young's modulus of these composites matched well with the values of the Young's modulus obtained from classical models [9] for composites filled with spherical inclusions; as shown in Fig. 2 for a test speed of 1 mm/min. For that comparison the Kerner-Nielsen's equation was used:

$$E_c = E_m\left(\frac{1+ABV_p}{1-BV_p}\right) \tag{6}$$

in which

$$A=\frac{7-5\nu_m}{8-10\nu_m} \qquad B=\frac{E_p/E_m-1}{E_p/E_m+A} \tag{7}$$

And also the Lewis-Nielsen model:

$$E_c = E_m\left(\frac{1+ABV_p}{1-B\psi V_p}\right) \quad \text{with} \quad \psi = 1-\exp\left(\frac{-V_p}{1-(V_p/V_p^{max})}\right) \tag{8}$$

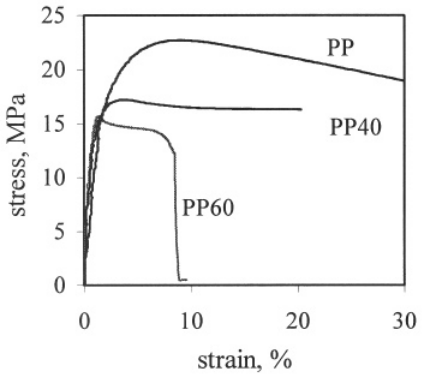

Fig. 2. Tensile curves at 10 mm/min.

Table 2. Tensile characteristics

Material	*Test speed* (mm/min)	*E* (GPa)	σ_y (MPa)
PP	1	1.10	20.1
	10	1.21	22.8
	100	1.49	25.3
PP40	1	150	17.3
	10	1.78	17.2
	100	1.93	19.8
PP60	1	2.18	14.7
	10	3.06	15.6
	100	3.65	15.8

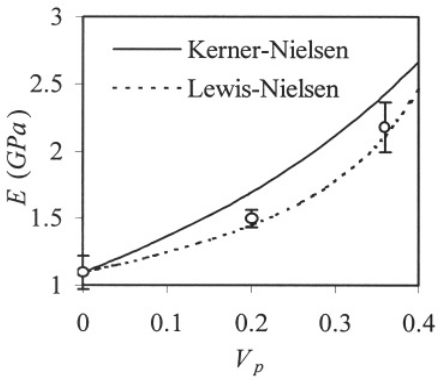

Fig. 2. Experimental values of E and Kerner's equation based models.

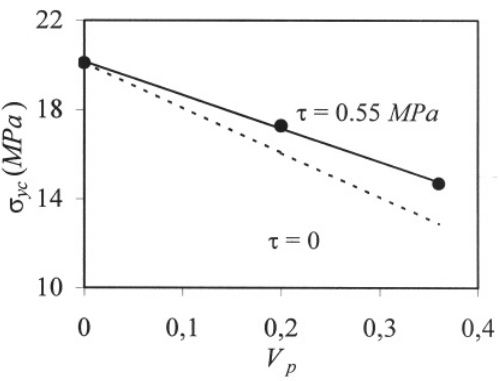

Fig. 3. Experimental values of σ_{yc} fitted according to equation (9).

In these expressions, *c*, *m* and *p* refer to the composite, matrix and particles respectively. The matrix Poisson's ratio (v_m) was taken equal to 0.42 [10], the filler Young's modulus (E_p) 64 GPa [11] and the filler maximum packaging fraction (V_p^{max}) 0.5 [12].
The observed decreasing trend of the composite yield stress (σ_{yc}) *versus* the filler content seems to agree with the trend predicted by the theoretical model for composites filled with fibres shorter than the critical length [13]. In this case, the load transmission mechanism acting between matrix and filler is only the interfacial shear:

$$\sigma_{yc} = \sigma_{ym}(1 - V_p) + 2\tau V_p \frac{l}{d} \tag{9}$$

In order to apply this model to our particulate filled system we have used, as a value of the fibre aspect ratio (*l/d*), the ratio between the plate equivalent diameter and the particle average thickness. The σ_{yc} values obtained at 1 mm/min and fitted to this theoretical model are shown in Fig. 3 and, as a result, a value of the interfacial shear strength (τ) of 0.55 MPa, is obtained, which means a real but low adhesion level between the PP copolymer and the Mg(OH)2 particles.

Fracture behaviour
The resistance *J-R* curves of the three materials under study are shown in Fig. 4, and the numerical results are summarised in Table 3. A decreasing trend of the critical *J* values has been obtained as the filler content increases in the composite, which indicates that magnesium hydroxide particles reduce the polymer resistance to crack growth initiation. This trend is in good agreement with that obtained in talc-filled [3] and short glass fibre-reinforced [4] PP homopolymer, although the J_{IC} values of PP homopolymer based composites are found to be lower than those obtained for PP copolymer based ones. This is due to the lower yield strength and higher ductility of PP copolymers, what allows absorbing more strain energy than the PP homopolymer during the fracture.
The observation of the fracture surfaces by SEM revealed that the crack propagation occurs within matrix ductile tearing. Firstly, microvoids are nucleated in the weakest points of the material, which are the intercrystalline regions in the case of the unfilled copolymer and the particle/matrix interface mainly in the case of the filled samples. The polymer between contiguous microvoids elongates progressively by plastic flow, causing micronecking, and the crack propagates thanks to the progressive failure of this drawn

polymer. On the fracture surface, the elongated matrix reminds fibrils or crests when observed by SEM (Fig. 5) the amount of which seems to increase as the $Mg(OH)_2$ content does and, at the same time, their elongation level decreases. On the basis of the morphological differences observed on the fracture surfaces, the decreasing trend of the fracture toughness values versus the filler content in the composite can be easily explained:

The amount of fibrils on the unfilled PP fracture surface (Fig 5.a) is the lowest of the three studied materials, and the fibril average thickness is found to be the highest. Both characteristics associated with the PP fracture mechanism are in accordance with both the low density of weak points able to nucleate microvoids and the high yield strength of the unfilled PP copolymer with regard to the filled samples. So, the fibrils in the PP60 fracture surface are the thinnest and the least elongated of the three samples (Fig. 5.c), what seems to be due to its high fraction of particles which easily promote the nucleation of microvoids and limit the polymer plastic flow. The morphology of the PP40 fracture surface appears as an intermediate case between PP and PP60, as it happens with the fracture toughness values.

The value of the tearing modulus increased with the filler content in the composite, indicating a higher resistance to crack growth once J_{IC} was reached. The cause could be the constraint of the polymer plastic flow provoked by the dispersed $Mg(OH)_2$ particles present in the filled samples. The obtained T_M values confirm the stability of the crack propagation observed during the test conducting of the three studied materials, because they fulfil the condition given by Paris [8] for a steady-state tearing:

$$T_M > \frac{2(D-a_0)^2 S}{D^3} \tag{10}$$

where the term on the right is the so-called applied tearing modulus, which value is 2 for the used test geometry.

It must be noted that the values of the material yield stress obtained from TPB test on the prismatic 6.35 mm thick specimens (Table 3) were found to be almost twice as much as those obtained by tensile test on the standard 3.175 mm thick specimens. In this sense, Wu [14] stated that the transition from plane-stress to plane-strain conditions in polymeric materials provokes that the material yield stress is two-folded. Therefore, one could accept, in a first approximation, that the crack tip in the 6.35 mm thick SENB specimens used in the J-integral fracture tests in under a plane-strain stress state. We think that could be more accurate to employ the yield stress value from the TPB test instead of that obtained from tensile test to determine the material blunting line (eq. (4)) and so the J_{IC} value. However, the unfilled PP copolymer did not fulfil the specimen thickness requirements usually applied to guarantee a plane-strain state along the crack front in metallic SENB specimens:

$$b, (D-a_0), D \geq \frac{25\, J_{IC}}{\sigma_y} \tag{11}$$

Then, although the J_{IC} value obtained for the unfilled PP sample (14.7 kJ/m^2) is in good agreement with the value reported by Hashemi and Williams [7] for a PP copolymer under plane-strain conditions (15.5 kJ/m^2), we can not assign that value as a PP property independent of the specimen size. In the case of $Mg(OH)_2$ filled PP samples the specimen thickness used was enough to satisfy that criterion.

Finally, the obtained J_{IC} values of the three materials were found to be smaller and therefore more conservative to design criteria than the $J_{0.2}$ ones. In this sense, we think that the blunting line is a more accurate criterion for fracture toughness evaluation of PP based composites than the J value taken at 0.2 mm of the total crack growth.

Table 3. Results of the TPB test and fracture parameters from the *J*-integral test.

Material	*Elasticity modulus*	*Yield strength*	*Fracture toughness*		*Tearing modulus*
	E^{TPB} (GPa)	σ_y^{TPB} (MPa)	$J_{0.2}$ (kJ/m^2)	J_{IC} (kJ/m^2)	T_M
PP	0.852	38.3	15.1	14.7	30.3
PP40	1.266	31.9	9.3	4.4	55.9
PP60	1.794	25.6	5.3	3.1	62.5

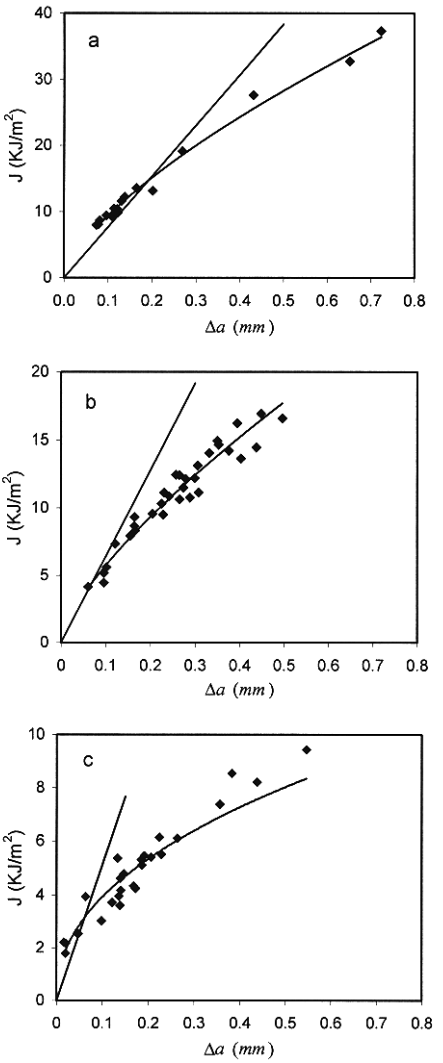

Fig. 4. J-R curves for (a) PP, (b) PP40, (c) PP60.

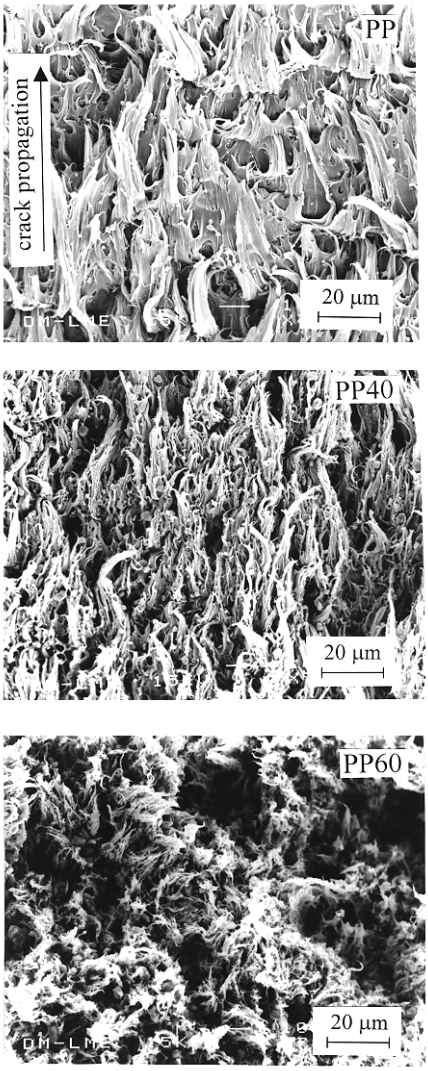

Fig. 5. Fracture surfaces by SEM.

Conclusions

The fracture behaviour of magnesium hydroxide filled polypropylene block copolymer has been investigated.

The main crack propagation mechanism identified in these materials is ductile tearing, which is initiated by microvoids nucleation at the interfacial sites. This mechanism is found to be more marked in the filled samples, due to their weak particle/matrix interface. In this sense, the Mg(OH)2 particles act as internal defects in the polymer and, as the magnesium hydroxide volume fraction is raised in the composite, a decrease of the resistance to crack growth initiation (fracture toughness) could be observed. Nevertheless, the presence of the filler particles limits to the matrix plastic flow during the material fracture process, which results in higher resistance to crack growth after the fracture onset as the filler volume fraction increases in the composite.

The Young's modulus of these composites can be predicted using models based in the Kerner equation and the yield strength by approximation to composites filled with fibres shorter than the critical length.

Acknowledgements

One of the authors (C. Morhain) thanks the CIRIT (Generalitat de Catalunya, Spain) for the concession of a predoctoral grant.

References

[1] Rothon RN, Hornsby PR (1996) Polym Degr Stab 54:383
[2] Xavier SF, Schultz JM, Friedrich K (1990) J Mat Sci 25:2411
[3] Velasco JI, de Saja JA, Martínez AB (1997) Fatigue Fract Engng Mater Struct 20:659
[4] Karger-Kocsis J (1993) J Polym Engng 12:77
[5] Begley JA, Landes JD (1972) Fracture Toughness, ASTM STP 514, American Society for Testing and Materials, Philadelphia.
[6] ESIS Technical Committee 4 (March 1991) A testing protocol for conducting J-R curve test on plastics. European Structural Integrity Society (ESIS).
[7] Hashemi S, Williams JG (1986) Polym. Eng. Sci. 11:760
[8] Paris PC, Tada H, Zahoor A, Ernst H (1979) Elastic Plastic Fracture, ASTM STP 668, American Society for Testing and Materials, Philadelphia.
[9] Lewis TB, Nielsen LE (1970) J Appl Polym 14:1449
[10] Vollenberg PHT, Heikens D (1989) Polymer 30:1656
[11] Jancar J (1989) J Mat Sci 24:3947
[12] Liauw CM, Lees GC, Hurst SJ, Northon RN, Dobson DC (1995) Plast Rubb Comp Proc Appl 24:249
[13] Hull D (199?) Materiales Compuestos, Reverte, Madrid.
[14] Wu S (1988) J Appl Polym Sci 35:549